

Flow velocity and boundary effects on fish interaction

*Original*

Flow velocity and boundary effects on fish interaction / Mozzi, Gloria; Comoglio, Claudio; Manes, Costantino. - In: SCIENTIFIC REPORTS. - ISSN 2045-2322. - 15:1(2025). [10.1038/s41598-025-13332-5]

*Availability:*

This version is available at: 11583/3008357 since: 2026-03-09T08:56:33Z

*Publisher:*

Nature

*Published*

DOI:10.1038/s41598-025-13332-5

*Terms of use:*

This article is made available under terms and conditions as specified in the corresponding bibliographic description in the repository

*Publisher copyright*

(Article begins on next page)



## OPEN Flow velocity and boundary effects on fish interaction

Gloria Mozzi<sup>1,2✉</sup>, Claudio Comoglio<sup>3</sup> & Costantino Manes<sup>3</sup>

How do environmental cues shape the coordination rules underlying collective motion in fish shoals? This question is crucial as freshwater migratory fish are globally declining due to river fragmentation, and collective motion is known to influence the effectiveness of fish pass solutions. However, experimental data on individual interactions and the effects of solid boundaries and hydrodynamic conditions remain limited. Adopting a reductionist approach - using fish pairs as the minimal shoal's unit - we examined how mean flow velocity and boundary proximity affect interaction dynamics in a riverine species. Towards this end, we tracked pairs of Italian riffle dace (*Telestes muticellus*) across three bulk flow velocities (2, 4 and 7 BL/s) and four regions in a confined open channel flow. We found shoaling time to be flow-invariant; however, fish shifted from side-by-side to in-line formations as flow increased, especially near walls. Correlation analysis revealed stronger velocity coupling at short distances (<6 BL) that remain largely stable across flow velocities. Response times differed by coordination direction: longitudinal responses (~0.5 s) were flow-invariant and symmetrical between lead and rear fish, while lateral responses primarily involved the rear fish reacting to the front one, and accelerated with increasing flow. Longitudinal coordination emerged only near side walls and in the central region, whereas lateral coupling peaked in central areas and strengthened with increasing flow. These findings reveal how physical context shapes coordination in riverine fish and provide empirical insights for fish pass design and fish movement modelling.

**Keywords** Fish movement, Collective behaviour, Hydrodynamics, Fish interaction, Fish passage

Coordinated collective motion is a swarm intelligence phenomenon arising from local interactions among individuals without a centralised control. Flocking birds, swarming ants and schooling fish all exhibit complex group-level behaviour emerging from simple, decentralised rules<sup>1</sup>. Understanding these principles is key to modelling natural systems and designing artificial ones, such as bio-inspired robotic swarms and Agent-Based Models (ABMs) of animal movement<sup>2,3</sup>.

In migratory freshwater fishes, collective coordination is crucial in upstream river navigation, which is often fragmented by dams, weirs and other artificial barriers<sup>4</sup>. Many fish species migrate in coordinated groups<sup>5</sup> and characterising their interaction rules can better inform conservation efforts, such as designing fish passage solutions that reconnect disrupted migratory routes<sup>6,7</sup> through adaptive and flow-aware ABMs that could simulate migration pathways under different design scenarios.

Key metrics to quantify shoal dynamics include shoaling time (i.e., time fish spend within a defined threshold distance from one another<sup>8–10</sup>, relative positioning<sup>11,12</sup> and interactions (quantifiable with methods that range from simple linear correlation analysis<sup>13,14</sup> to more sophisticated techniques like transfer entropy<sup>15,16</sup>. For riverine fish, these aspects can be heavily modulated by the hydrodynamic environment (as reviewed in Mozzi, Manes, et al., 2024<sup>7</sup>). Despite this, how individuals integrate social and hydrodynamic information remains fragmented or poorly understood, particularly concerning the effects of mean flow velocity ( $U_B$ , typically intended either as a local time- and depth-averaged velocity or, as in most laboratory studies, a bulk velocity obtained from the ratio between the measured discharge and the cross sectional area of open channel flows) and river boundaries on shoal dynamics<sup>17</sup>.

Previous studies on flow velocity's impact on fish shoaling times have yielded conflicting results. Guppies (*Poecilia reticulata*) displayed reduced shoaling time with increasing flow velocity<sup>10</sup> whereas wild zebrafish (*Danio rerio*), chubs (*Leuciscus cephalus*), and minnows (*Phoxinus phoxinus*) showed increased shoaling tendency with increasing  $U_B$ <sup>8,9,11</sup>. Notably, most of these studies have consistently defined shoaling as fish being within four Body Lengths (BL) of each other, and although this threshold is widely accepted for standing waters<sup>14,18,19</sup> its a priori applicability in running waters is questionable.

<sup>1</sup>CMCC Foundation - Euro-Mediterranean Center on Climate Change, Venice, Italy. <sup>2</sup>Ca' Foscari University of Venice, Venice, Italy. <sup>3</sup>Department of Environment, Land and Infrastructure Engineering, Politecnico di Torino, Torino, Italy. ✉email: gloria.mozzi@cmcc.it

Regarding the effect of flow velocity on swimming formation, several studies have found that fish tend to adopt a side-by-side configuration at relatively high flow velocities<sup>11,12,20,21</sup>. In contrast, Li et al. (2020)<sup>2</sup> observed that rear fish position themselves at an angle from the leader, exploiting the vortices created by the leader's tailbeat. They hypothesised that energetic benefits in school formation arise from spatial formation and tailbeat synchronisation ("vortex phase matching"). However, all the mentioned studies examined velocity ranges below 4.5 BL/s<sup>12,20</sup> which do not reflect conditions of natural rapids or engineered fishways<sup>22,23</sup>.

Experimental observations on the effect of flow velocity on fish interaction in shoals are also limited. Chicoli et al. (2014)<sup>24</sup> found that giant danio (*Devario aequipinnatus*) exhibited stronger mutual responses in still water than in flowing conditions, likely due to weaker lateral line signals masked by ambient flow. De Bie et al. (2020)<sup>11</sup> found that information transfer between minnow pairs (*Phoxinus phoxinus*) predominantly flowed from front to back, with no significant differences between velocity treatments. They also identified peaks in velocity cross-correlation functions to determine the timescale over which fish responded, ranging from 0.3 to 0.5 s, with no reported differences between velocity treatments.

Ultimately, nearly all previous works either simulated or observed shoaling behaviour in open waters, neglecting the potential impact of boundaries such as side walls or riverbanks. In these areas, reduced flow velocities allow fish to save energy<sup>25</sup> and several species are known to exploit this by swimming along riverbanks during migration<sup>25–27</sup>. Boundaries can affect group behaviour by acting as an additional attraction force<sup>28</sup> and to our knowledge, no study has investigated the effect of boundaries on fish interactions in running waters.

This work aims to investigate shoal formation and interaction at flow velocities ranging from 2 to 7 BL/s in a confined swimming arena, thereby accounting for boundary effects. Adhering to the reductionist approach<sup>11,14,20</sup> we analyse fish pair trajectories at three flow conditions across four flume regions. This deliberate choice aligns with the requirement to measure fundamental interaction metrics, focusing on the simplest subsystem of a shoal, namely fish pairs. Our objective is to characterise shoaling based on (i) shoaling time, (ii) fish mutual positioning, and (iii) correlation of fish velocities and their dependence on fish relative distance, orientation, presence of boundaries, and time lags. We hypothesise that flow velocity and boundaries significantly affect collective behaviour, shaping shoal structure and interactions. Our findings aim to advance the understanding of how environmental factors shape fish interaction rules. These rules offer valuable insights into shoal decision-making processes<sup>29</sup> as well as empirically grounded input for ABMs of fish movement and the broader modelling of coordinating systems.

## Materials and methods

### Animals, experimental protocol, trajectory data

Italian ruffle dace (*Telestes muticellus*) is a social fish species native to the streams and rivers of the Italian peninsula, which, despite its abundance, has been relatively understudied<sup>30</sup>. This study involved a cohort of 20 wild juvenile Italian ruffle dace, with an average length of 5.14 cm (SD ± 0.34 cm). Fish were captured by electrofishing along approximately 1 km of the Noce Stream in northern Italy (44°56'18.52" N, 07°23'11.24" E) in May 2021. Following capture, individuals were transported to a nearby hatchery and later used in experiments conducted in an open-channel flume with transparent walls. Further details on capture, transfer, housing, and feeding procedures are provided in Mozzi et al. (2024)<sup>31</sup>. The flume was equipped with a combined pump-inverter system, enabling precise control over flow rate and a downstream weir of adjustable height, allowing for control over flow velocity and water depth. The test section measured 60 × 30 × 15 cm<sup>3</sup> (length × width × depth) and was delimited by an upstream honeycomb grid (cell size of 0.5 cm) and a downstream grid (mesh size of 0.5 cm). Two cameras were positioned at the bottom and side to record the experiments on the horizontal and vertical planes, respectively (Sony FDR-AX43; 1920 × 1080 pixels, 50 fps). Further details regarding the animals and the experimental setup can be found in the Supplementary Material and in Mozzi et al. (2024)<sup>31</sup>.

The experimental protocol entailed introducing fish pairs into the flume with a bulk flow velocity ( $U_B$ ) of 10 cm/s ( $U_{B10}$ , i.e. 2 BL/s). This flow velocity was kept constant for 15 min, divided into an initial 5-minute habituation period followed by a 10-minute trial period. Subsequently, the flow velocity was incrementally raised to 20 cm/s ( $U_{B20}$ , i.e. 4 BL/s), and maintained at this level for an additional 10 min. Finally, pairs were exposed to the highest flow velocity of 35 cm/s ( $U_{B35}$ , i.e. 7 BL/s), for 10 min.

The selected velocity range was intended to span from energetically manageable conditions ( $U_{B10}$ ) to flows posing moderate ( $U_{B20}$ ) and high ( $U_{B35}$ ) locomotor challenges. Ashraf et al. (2024)<sup>32</sup> tested swimming performance in individual fish of the same species and size class, showing that at 45 cm/s, all individuals fatigued within 2 min, whereas at 35 cm/s, over 20% were able to swim more than 30 min. These findings suggest that a flow velocity of 35 cm/s (7 BL/s) poses a significant challenge without leading to fatigue within the trial duration.

Water depth was maintained at 15 cm throughout the experiment, with a water temperature of 14 °C (SD ± 0.3 °C). The analysis of vertical positioning indicated that fish remained within the lower 5 cm of the water column, just above the flume bottom, for more than 70% of the time. This behaviour allowed us to approximate their trajectory as two-dimensional within the horizontal plane.

### Overview of data analysis

To avoid including transient behaviours resulting from changes in flow velocity, only the last 7 min of each 10-minute velocity trial were analysed, with the first 3 min after the velocity transient discarded to allow fish to stabilise their behaviour. The fish's positional data (expressed in cm, with a precision of ± 3 mm) was obtained using a custom-trained convolutional neural network (CNN) model (YOLOv4)<sup>33</sup> a deep learning architecture widely used for object detection. The CNN, trained on 10,000 annotated images to detect fish heads, achieved 96% accuracy in both mAP50 and F1 score. The detected positions were then processed using a Kalman filter-based tracking algorithm to reconstruct individual fish trajectories. Further details on the tracking methodology are available in Mozzi et al. (2024)<sup>31</sup>.

The reference system was defined with its origin at the head of the Leading fish (L). The x-axis was aligned with the flow direction, while the y-axis was oriented transversely to the water flow within the horizontal plane (Fig. 1). Fish trajectories were analysed to compute shoaling times, mutual positioning of fish, and cross-correlation functions, as described in the section below. Cross-correlation functions were used to quantify fish interactions across various relative distances, orientations and swimming regions. These functions also allowed for estimating decorrelation distances ( $D_d$ , i.e., distance up to which fish interact) and response times ( $t_r$ , i.e. the time after which a fish, on average, responds to the movement of the other fish).

The arena was partitioned into four distinct swimming regions (SR): Back, Front, Centre, and Side (Fig. 1). The Front and Back regions were delineated as areas within a 5 cm (equivalent to 1 BL) distance from the upstream and downstream grids, respectively. The Side region was defined as the lateral area located within 2.5 cm (equivalent to 0.5 BL) from the side walls, excluding the Front and Back regions. The Centre region was subsequently identified as the central area not included in the other defined boundary regions. These values were

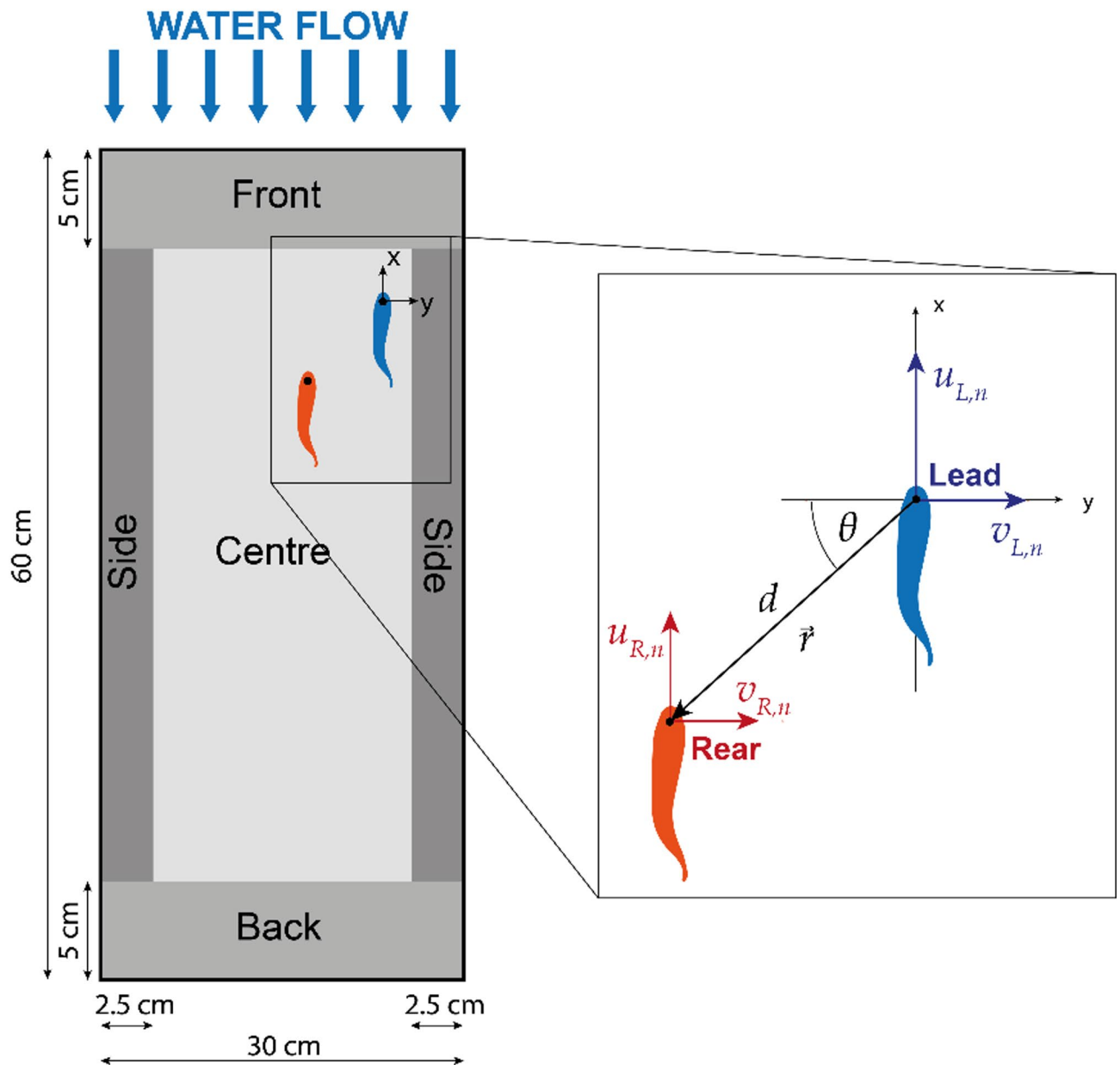


**Fig. 1.** Schematic representation of the bottom-view of the test section, along with the delimitation of the Swimming Regions (SR: Front, Centre, Side and Back) and coordinate reference system.  $u_{L,n}$  and  $u_{R,n}$  represent longitudinal velocities for the Lead and Rear fish of the  $n^{\text{th}}$  experiment, respectively, whereas  $v_{L,n}$  and  $v_{R,n}$  stand for the lateral ones.  $d$  is the distance between the two fish and  $\theta$  is the angle between them (defined as  $0^\circ$  for fish staying side-by-side and  $90^\circ$  when in an in-line configuration).  $\vec{r} = \begin{pmatrix} d \\ \theta \end{pmatrix}$  represents the vector distance between the two fish.

selected based on the results of the hydrodynamic characterisation of the flume - performed using a combination of Laser-Doppler-Anemometer measurements and Computational Fluid Dynamics simulations - as well as fish position analysis previously described in Mozzi et al. (2024)<sup>31</sup>. More specifically, the median distance from lateral walls at  $U_{B35}$  was found to be below 0.5 BL, while the median distance from the upstream or downstream at  $U_{B10}$  was below 1 BL.

### Cross-correlation functions

To quantify the interaction between fish pairs, we employed cross-correlation functions of fish velocity components along the longitudinal and lateral coordinates<sup>13,14</sup>. For clarity and conciseness, we present the methodology using the longitudinal component ( $u$ ) as an example. The same procedure was applied to the lateral component ( $v$ ), but its detailed formulation is omitted here to avoid redundancy. The fish with the lowest longitudinal coordinate (measured from the upstream grid) was designated as the Lead (L) fish, while the other as the Rear (R). This classification was justified by the observation that the fish remained primarily aligned with the flow direction for the entire duration of the experiments.

For each  $n^{\text{th}}$  experiment, the cross-correlation function with time lag  $\tau$  ( $c_{u,n}(\vec{r}, \tau)$ ) between the longitudinal velocity of the Lead fish ( $u_{L,n}$ ) and the Rear fish ( $u_{R,n}$ ) was estimated using the Pearson correlation coefficient - a widely used measure of linear relationship between two variables<sup>34</sup> - and computed as:

$$c_{u,n}(\vec{r}, \tau) = \frac{\sum_t (u_{L,n}(t) - \overline{u_{L,n}}) (u_{R,n}(\vec{r}, t + \tau) - \overline{u_{R,n}}(\vec{r}))}{\sqrt{\sum_t (u_{L,n}(t) - \overline{u_{L,n}})^2} \sqrt{\sum_t (u_{R,n}(\vec{r}, t + \tau) - \overline{u_{R,n}}(\vec{r}))^2}} \quad (1)$$

Where the overbar symbol refers to time averaging,  $t$  is time,  $\tau$  is a time lag,  $\vec{r} = \begin{pmatrix} d \\ \theta \end{pmatrix}$  represents the vector distance between the two fish, whereby  $d$  is the distance between the two fish and  $\theta$  is the angle between them, ranging from 0 to 90°, defined as 0° for fish staying side-by-side and 90° when in an in-line configuration (Fig. 1).

The mean correlation  $C_u$  was estimated from the ensemble average of the  $N$  experiments:

$$C_u(\vec{r}, \tau) \stackrel{\text{def}}{=} \frac{1}{N} \sum_{n=1}^N c_{u,n}(\vec{r}, \tau) \quad [N = 10] \quad (2)$$

To determine the spatial scale of fish interactions and quantify the decorrelation distance  $D_d$ , cross-correlation functions  $c_{u,n}(\vec{r}, \tau)$  with zero-time lag ( $\tau = 0$ ) were calculated at chosen relative distances between fish (i.e. at chosen distances  $d$  and regardless of  $\theta$ ). Specifically, data were discretised into two body length (BL) increments across the range of 0 to 14 BL, and the mean correlation  $C_u(d)$  was computed:

$$C_u(d) = \frac{1}{N} \sum_{n=1}^N c_{u,n}(d) \quad [2(i-1) < d < 2i, \tau = 0] \quad (3)$$

with  $i$  ranging from one to seven ( $i \in [1 \dots 7]$ ). A correlation threshold of 0.05 was set, designating any correlation values below this threshold as statistically insignificant. This threshold was selected based on a correlation analysis between the velocity time series of two unrelated fish associated with different randomly selected experiments, revealing that 95% of random correlations fell below 0.05. Employing a conservative approach, the decorrelation distance  $D_d$  was defined as the distance beyond which the mean correlation coefficient remained consistently below 0.05 for each velocity component and  $U_B$  (i.e.,  $C_u(d \geq D_d) < 0.05 \forall U_B$  and  $C_v(d \geq D_d) < 0.05 \forall U_B$ ). For all analyses further described, this decorrelation distance was employed as a threshold to filter out the time intervals in which fish were considered too far apart to interact.

The effect of relative orientation on fish interactions was assessed by computing zero-lag correlation functions  $c_{u,n}(\vec{r}, \tau = 0)$  at time intervals when the fish were positioned at specific intervals of  $\theta$  (ranging from 0° to 90° in 15° increments), and a relative distance below the decorrelation distance  $D_d$ :

$$C_u(\theta) = \frac{1}{N} \sum_{n=1}^N c_{u,n}(\theta) \quad [\pi/12(i-1) < \theta < \pi/12i; d < D_d; \tau = 0] \quad (4)$$

with  $i$  ranging from one to six ( $i \in [1 \dots 6]$ ).

In order to examine the effect of the swimming regions ( $SR$ ),  $N$  cross-correlation functions were computed for each  $SR_i$  ( $SR_i \in [\text{Back}, \text{Centre}, \text{Front}, \text{Side}]$ ), at a zero-time lag and a relative distance below the decorrelation distance  $D_d$ :

$$c_{u,n}(SR) = c_{u,n}(SR_i) \quad [d < D_d; \tau = 0] \quad (5)$$

Cross-correlation functions across different time lags  $\tau$  ( $C_u(\tau)$ ) were computed for any  $\vec{r}$ , where the relative distance ( $d$ ) was less than the decorrelation distance  $D_d$ :

$$C_u(\tau) = \frac{1}{N} \sum_{n=1}^N c_{u,n}(\tau_i) \quad [d < D_d] \quad (6)$$

With  $\tau_i \in [-5 \dots 5]$  s with step intervals of 0.02 s for  $|\tau| \leq 0.1$  s, 0.1 s for  $0.1 < |\tau| \leq 0.5$  s, and 1 s for  $1 < |\tau| \leq 5$  s).

$$t_{r,u} = \frac{1}{N} \sum_{n=1}^N \tau_{MAX,u,n} \quad (7)$$

With  $\tau_{MAX,u,n}$  defined as the time lag in which the maximum correlation occurs:

$$\tau_{MAX,u,n} : c_{u,n}(\tau_{MAX}) = \max_{\tau} (c_{u,n}(\tau ; d < D_d)) \quad (8)$$

### Statistical analysis

Data analysis was carried out using R version 4.0.5<sup>35</sup>. Plots were generated using the *ggplot2* package (version 3.4.0<sup>36</sup>), and statistical analysis was performed using the *rstatix* package (version 0.7.0<sup>37</sup>) in R, with a significance threshold set at  $p < 0.05$ . Response times ( $t_{r,u}$ ,  $t_{r,v}$ ) exhibited non-normal distributions based on the Shapiro-Wilk test ( $p$ -value  $< 0.05$ ). Consequently, the Friedman test was employed to assess the impact of flow velocity as a within-subject factor, accounting for repeated measures across varying  $U_B$ <sup>38</sup>. The Friedman test was also applied to evaluate the effect of *SR* on fish velocity correlations ( $c_{u,n}(SR)$  and  $c_{v,n}(SR)$ ), which also showed non-normal distributions (Shapiro-Wilk test:  $p$ -value  $< 0.05$ ). A statistical analysis of shoaling time and swimming region usage was also performed, as described in the Supplementary Information.

### Ethical approval

The study was conducted following the Declaration of Helsinki and under the ARRIVE guidelines<sup>39</sup>. The study protocol was approved by the Protection of Flora and Fauna Department of the Metropolitan City of Turin (authorised by D.D. n.4457 of 29 October 2020) and conducted in accordance with the relevant guidelines and legislation under the provisions of Art.2 of the national Decree n.26/2014 (implementation of Dir. 2010/63/EU). All possible appropriate measures were taken to ensure fish welfare during collection, housing, handling, and testing.

## Results

### Shoaling time and swimming region usage

Shoaling time is found to be statistically unaffected by  $U_B$ , irrespective of the threshold distance applied to consider fish shoaling (Friedman test:  $p$ -value  $> 0.05$  for 1, 2, 4, 6, and 8 BL). Specifically, for a threshold distance of 4 BL, average shoaling times (mean  $\pm$  standard deviation) constitute  $79\% \pm 35\%$ ,  $85\% \pm 32\%$ , and  $83\% \pm 30\%$  of the total time in the flume for  $U_{B10}$ ,  $U_{B20}$ , and  $U_{B35}$  respectively (see Supplementary Information for further details on shoaling time analysis).

The analysis of the time spent by fish in each region reveals that at  $U_{B10}$ , fish predominantly occupied the Front region (see Supplementary Information), occasionally attempting to swim through the honeycomb grid. At  $U_{B20}$ , the distribution was more even, while at  $U_{B35}$ , fish primarily swam next to the lateral walls, specifically in the Side region. Statistical analyses confirm that at  $U_{B10}$  and  $U_{B35}$ , fish tended to swim in specific regions, while this was not statistically significant at  $U_{B20}$  (see Supplementary Information). The analyses also indicate that the  $U_B$  significantly influenced the utilisation of the Front, and Side regions by fish.

### Mutual positioning

Analysis of the mutual positioning within the entire flume region reveals distinct patterns: at  $U_{B10}$  and  $U_{B20}$ , fish tended to adopt a side-by-side configuration, while at  $U_{B35}$ , an in-line configuration was prevalent (Fig. 2). In trials where fish differed noticeably in size (i.e., the difference was apparent to the human eye), no consistent pattern was observed regarding the larger individual occupying either the Front or Rear position.

### Relative distance and orientation effects on fish interaction

The mean longitudinal cross-correlation function computed over different relative distances,  $C_u(d)$  displays positive values, albeit lower than 0.2 (Figs. 3 and 4a). Such values drop below 0.05 when the distance between fish exceeds 5 BL for  $U_{B10}$  and  $U_{B35}$ , while for  $U_{B20}$ , they drop beneath this value for  $d \geq 6$  BL. For the lateral velocity component,  $C_v(d)$  drops below the threshold value at 3 BL for  $U_{B35}$ , 4 BL for  $U_{B10}$ , and 6 BL for  $U_{B20}$  (Fig. 4b). For the following analysis, we conservatively used 6 BL as decorrelation distance  $D_d$ .

The effects of relative orientation on fish interaction are captured by  $C_u(\theta)$  and  $C_v(\theta)$  (i.e., mean longitudinal and lateral cross-correlation functions computed over different relative orientations, Fig. 4c and d, respectively). The longitudinal component  $C_u(\theta)$  exhibits a trend for  $U_{B10}$ , displaying an increasing correlation with increasing  $\theta$ , reaching above 0.25 when fish displayed an in-line configuration. A similar but less pronounced behaviour is observed at 20 cm/s. At  $U_{B35}$ , the correlation exhibits no discernible trend, remaining consistently below 0.15. Conversely, the lateral component  $C_v(\theta)$  displays opposite trends at  $U_{B10}$  and  $U_{B20}$ , reaching the largest values at  $\theta = 0^\circ$  (side-by-side formation) and registering correlations of 0.3 and 0.25 for  $U_{B20}$  and  $U_{B10}$ , respectively. These correlations gradually decrease, falling below 0.15 at higher angles (i.e. approaching an in-

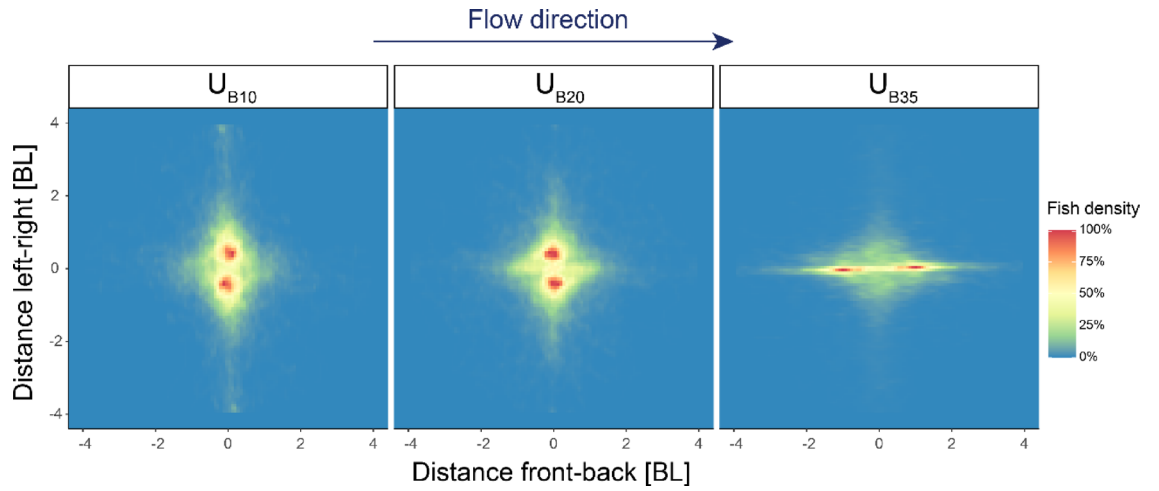


**Fig. 2.** Mutual position of fish pairs for different flow velocities  $U_{B10}$ ,  $U_{B20}$ , and  $U_{B35}$  (10, 20 and 35 cm/s of bulk velocity, and 2, 4 and 7 BL/s, respectively).

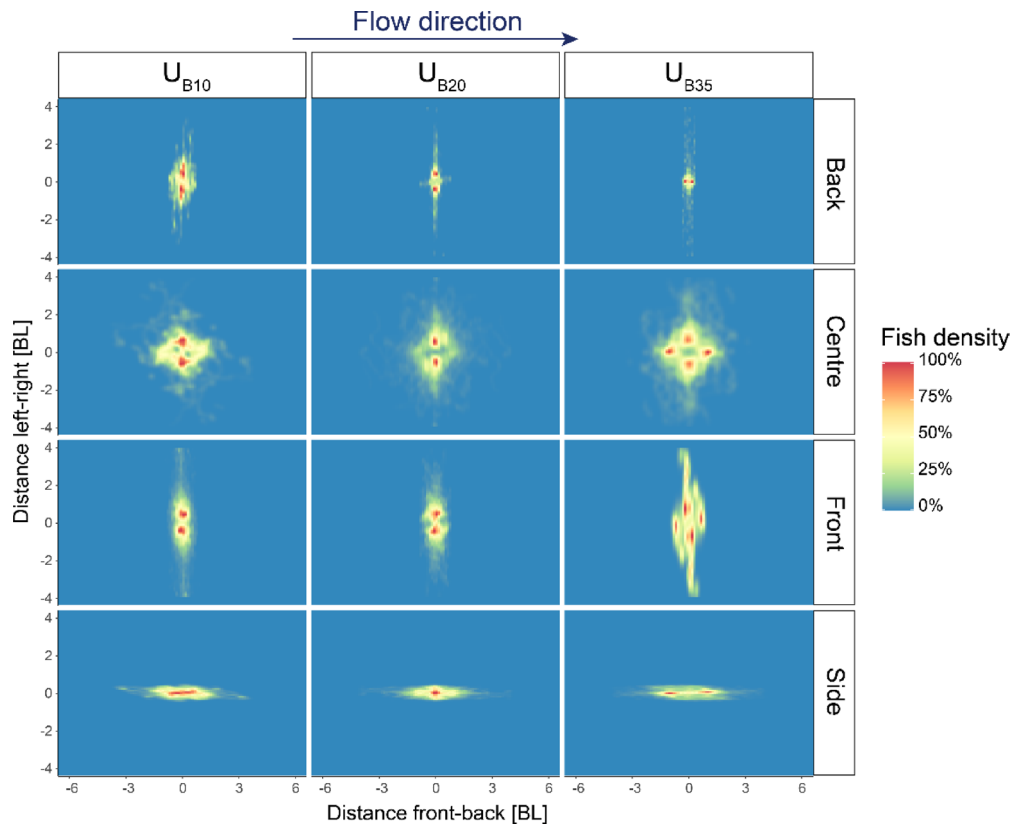


**Fig. 3.** Mutual positions of fish pairs for different swimming regions (*SR*) and different bulk flow velocities  $U_B$  ( $U_{B10} = 10$  cm/s,  $U_{B20} = 20$  cm/s and  $U_{B35} = 35$  cm/s). “Front” and “Back” regions are defined as areas located within 5 cm (1 BL) of the upstream and downstream grid, respectively. “Side” regions are defined as areas within 2.5 cm (0.5 BL) from lateral walls, remaining at least 5 cm from upstream/downstream grids. The “Centre” region refers to the central area, which does not overlap with any other defined regions. Water is flowing from left to right for all panels.

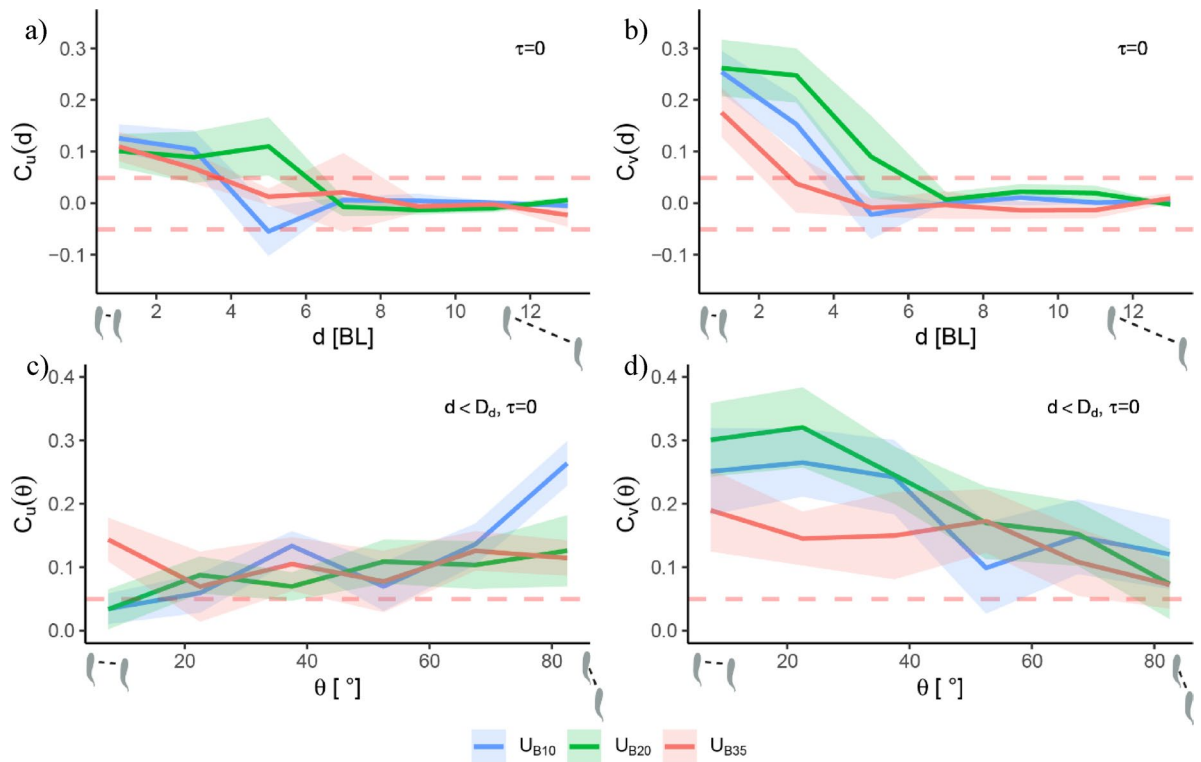


**Fig. 4.** Mean zero-time lag ( $\tau = 0$ ) correlation between fish velocities for the three flow velocities  $U_B$  ( $U_{B10} = 10$  cm/s in blue,  $U_{B20} = 20$  cm/s in green and  $U_{B35} = 35$  cm/s in red). Top panels are for correlation for different distances between fish on the longitudinal (**a**,  $C_u(d)$ ), and lateral (**b**,  $C_v(d)$ ). Bottom panels represent correlation for different orientations in (**c**,  $C_u(\theta)$ ) and (**d**,  $C_v(\theta)$ ).  $\theta = 0^\circ$  corresponds to a side-by-side configuration, while  $\theta = 90^\circ$  stands for an in-line arrangement. The coloured bands represent the standard deviation ( $N = 10$  experiments), and dashed red lines represent the threshold for non-significant correlation ( $< 0.05$ ).

line configuration). In the case of  $U_{B35}$ , a similar trend is observed, albeit generally lower, with the maximum correlation staying below 0.2 for  $\theta = 0^\circ$ .

### Boundary regions effects on interactions

To assess whether boundary effects influenced interactions between pairs, we calculated  $N$  (10) zero-time lag ( $\tau = 0$ ) correlation functions on the longitudinal ( $c_{u,n}(SR)$ ) and lateral ( $c_{v,n}(SR)$ ) velocity components for each swimming region ( $SR$ , Fig. 5). Significant longitudinal correlation (i.e., with a median higher than 0.05) was observed only in the Centre and Side regions (Fig. 5a), and at  $U_{B20}$ , a significant correlation is found solely in the Side regions. Conversely, for lateral motion (Fig. 5b), a significant correlation is observed in the Centre and Front regions (except for  $U_{B35}$ , at which correlation is significant only in the Centre). Statistical analysis reveals that the effect of  $SR$  is significant across all  $U_B$  for both longitudinal and lateral motion (Table 1).

### Response time

Cross-correlation functions help to depict the response time of interaction by showing peaks in correlation at certain time lags ( $\tau$ ). Negative lags depict a correlation between the velocities of the Lead fish at the current time and the delayed velocity of the Rear fish (L responds to R). On the other hand, positive lags correspond to a delay in the Lead fish (R responds to L).  $C_u(\tau)$  shows two prominent peaks, one for the positive  $\tau$  and one for the negative (Fig. 6a). The peaks occur at lags of magnitude  $0.47 \pm 0.31$ ,  $0.47 \pm 0.44$ , and  $0.54 \pm 0.5$  s for flow velocities of  $U_{B10}$ ,  $U_{B20}$ , and  $U_{B35}$ , respectively. Statistical analysis reveals that  $U_B$  did not affect such response times (Friedman test:  $p$ -value  $> 0.05$ ). By contrast,  $C_v(\tau)$  displays only one major peak on the positive lags for all flow velocities (Fig. 6b). In this case, the peaks are located at  $0.73 \pm 0.49$  s lags for  $U_{B10}$ ,  $0.54 \pm 0.29$  s for  $U_{B20}$ , and  $0.28 \pm 0.12$  s for  $U_{B35}$ . Statistical analysis shows that  $U_B$  significantly affects the response time (Friedman test:  $\chi^2 = 6.1$ ,  $p$ -value = 0.047).

### Discussion

Understanding how flow velocity influences shoaling behaviour is critical for interpreting fish social dynamics under varying environmental conditions. However, existing studies report inconsistent findings: some works show increased shoaling time with increasing flow velocities<sup>8,9,11</sup> while others report the opposite<sup>10,40</sup>. For instance, De Bie et al. (2020)<sup>11</sup> found that minnow pairs (*Phoxinus phoxinus*) increased shoaling time with

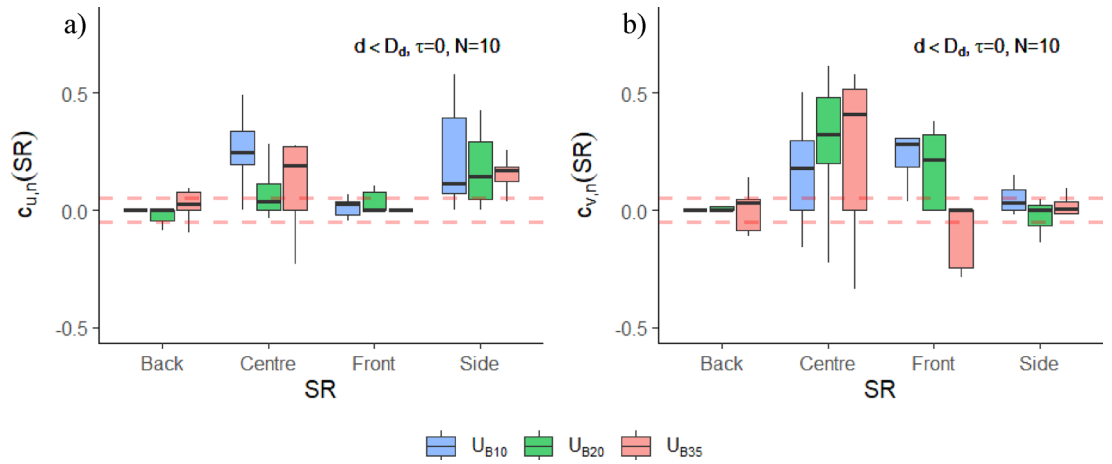


**Fig. 5.** Zero-time lag ( $\tau = 0$ ) correlation functions in different swimming regions (SR) on the longitudinal (a,  $c_{u,n}(SR)$ ) and lateral (b,  $c_{v,n}(SR)$ ) velocity components across the three bulk velocities:  $U_{B10} = 10$  cm/s (blue),  $U_{B20} = 20$  cm/s (green), and  $U_{B35} = 35$  cm/s (red). Here,  $n$  denotes the individual experiment index, with a total number of experiments  $N = 10$ . “Front” and “Back” regions are defined as areas located within 5 cm (1 BL) of the upstream and downstream grid, respectively. “Side” regions are defined as areas within 2.5 cm (0.5 BL) from lateral walls, remaining at least 5 cm from upstream/downstream grids. The “Centre” region refers to the central-area, which does not overlap with any other defined regions. Dashed red lines indicate the threshold for non-significant correlation ( $< 0.05$ ).

Factor	Cluster	$c_u(SR)$ ( $p$ -values)	$c_v(SR)$ ( $p$ -values)
SR	$U_{B10}$ (10 cm/s)	$< 0.001$	0.002
	$U_{B20}$ (20 cm/s)	0.001	0.005
	$U_{B35}$ (35 cm/s)	0.030	0.042

**Table 1.** Effect of swimming region (SR) on fish interaction on the longitudinal and lateral components ( $c_{u,n}(SR)$  and  $c_{v,n}(SR)$ , respectively). The analysis is conducted using the Friedman test ( $N = 10$  and  $df = 3$  for all tests).

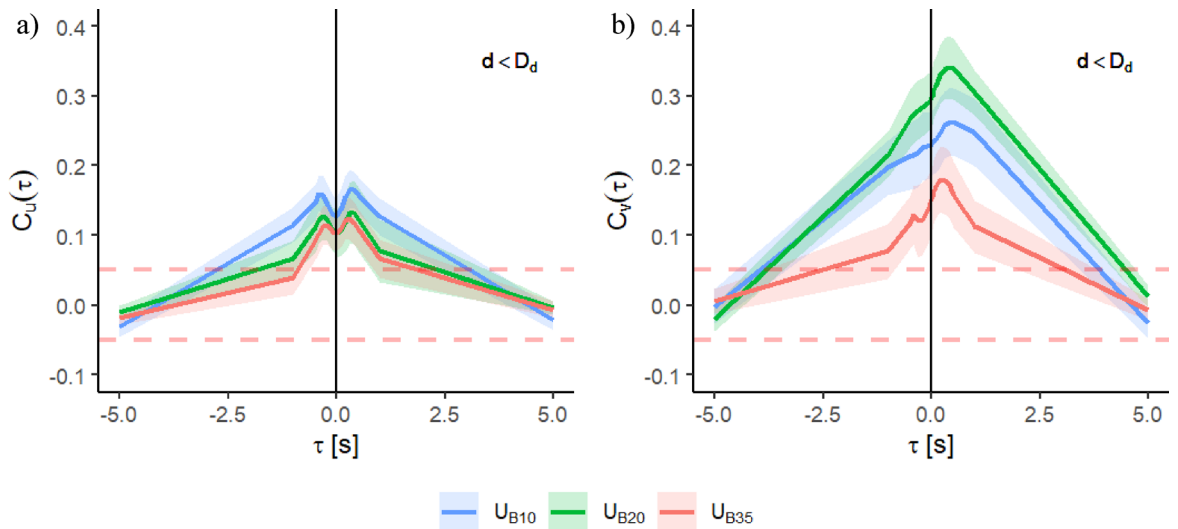


**Fig. 6.** Mean cross-correlation functions of longitudinal (a,  $C_u(\tau)$ ) and lateral (b,  $C_v(\tau)$ ) velocity time series between the Leading fish and the Rear fish for the three flow velocities. Positive lags ( $\tau$ ) means that the Lead is delayed (Rear responds to Lead), and negative lags represent the Lead fish responding to the Rear. The coloured bands represent the standard deviation ( $N = 10$  experiments), and dashed red lines represent the threshold for non-significant correlation ( $< 0.05$ ).

increasing flow velocity in a flume, although their analysis was restricted to the arena's central region and much lower velocities ( $< 2$  BL/s). In our case, the absence of a flow-dependent change in shoaling time across higher velocities suggests that hydrodynamic effects might saturate beyond a certain flow threshold, though this hypothesis should be tested for more fish species and a broader range of hydrodynamic conditions, including varying turbulence regimes.

Spatial positioning revealed flow-dependent preferences linked to hydrodynamic and behavioural trade-offs. At the highest velocity, fish tended to swim in-line in the Side region (specifically 56% of the time, see Supplementary Information), likely to reduce drag by exploiting slower flow near the walls - a phenomenon observed in studies involving single fish<sup>25,41,42</sup>. At the lowest flow velocity, fish preferred swimming side-by-side in the Front region (61% of the time), where low turbulence directly downstream of the honeycomb grid may offer an energy-saving benefit<sup>25</sup>. However, attempts to swim through the grid suggest that motivational factors beyond energy conservation may be at play. Indeed, low flows might mimic natural conditions that prompt drift-foraging, where fish linger in low-velocity zones alongside faster currents to capture drifting invertebrates, a behaviour observed in other benthic cyprinids, such as *Phoxinus phoxinus*<sup>43</sup>.

At intermediate velocity, fish showed no strong preference for any region, distributing uniformly throughout the arena. This pattern, previously reported by Mozzi et al. (2024)<sup>31</sup> coincided with peak exploration tendency and suggests that this velocity may represent a behavioural optimum, balancing hydrodynamic ease and spatial exploration.

The observed region-dependent shift from side-by-side to mixed or in-line formations with increasing flow velocity (Fig. 3) suggests that swimming formation is sensitive not only to hydrodynamic conditions, but also to spatial constraints. However, the observed pattern contrasts with previous findings by Ashraf et al. (2016, 2017)<sup>12,20</sup> who found a progressive preference for side-by-side ("phalanx") formation with increasing flow velocity. This behaviour was attributed to a strategy for optimising swimming performance whereby coordinated swimming enhances thrust and reduces tail beat frequencies, hence reducing energy expenditure.

The present study therefore indicates that the results by Ashraf et al. (2016)<sup>20</sup> do not seem to be of general validity. While the observed differences may be attributed to the different fish species used in this study and their study, we speculate that methodological differences could also play a significant role. In particular, Ashraf et al. (2016)<sup>20</sup> employed a narrower velocity range than our study ( $0.77 \div 4$  BL/s vs.  $2 \div 7$  BL/s). Note also that for  $U_{B10}$  (2 BL/s) and  $U_{B20}$  (4 BL/s) (i.e. within the range of velocities investigated by Ashraf et al. (2016)<sup>20</sup>, we report a preferred side-by-side configuration in most of the available space (Fig. 3), hence consistent with their results. It is at very challenging hydrodynamic conditions (i.e.  $U_{B35}$ , 7 BL/s) that we observe fish to display more preference to the in-line configuration. This is puzzling: if the side-by-side configuration provides optimal energy-savings, as argued by Ashraf et al. (2016)<sup>20</sup> why is it not consistently employed under more hydrodynamically challenging conditions? One possible explanation is that the side-by-side formation is not universally the most energetically advantageous at all flow velocities, as also observed by Li et al. (2020)<sup>2</sup>. Another possibility is that swimming formations are not solely governed by energy-saving purposes. Other factors, such as information transfer<sup>11</sup> stress response<sup>44</sup> or a combination of those, may also play a role. For example, De Bie et al. (2020)<sup>11</sup> observed a preference for side-by-side configuration at 2 BL/s and argued that this formation optimises information transfer, which is crucial for maintaining coordinated motion in shoals. The relative importance of these different drivers and their effect on fish interaction and swimming formations remains an open question.

Regarding the magnitude of interaction, we observed that it also varied with flow and positioning. Correlations in fish velocity remained significant up to a relative distance of 6 BL (Fig. 4a, b), though this result is contingent upon the threshold we defined for negligible correlation (in our case, 0.05). Interestingly, the maximum correlation occurs at  $U_{B20}$ , coinciding with the velocity at which fish exhibited the highest exploration rate<sup>31</sup>. Lateral correlation exceeded longitudinal at low and intermediate flow, but dropped sharply at  $U_{B35}$ , likely due to restricted lateral movement near walls. Orientation-based analysis (Fig. 4c, d) confirmed that in-line configurations - typically observed in the Side region - exhibit stronger longitudinal correlations, while side-by-side positioning supported lateral coordination, likely via visual cues.

The positioning of fish, influenced by flow conditions, significantly shaped their interactions with one another. At lower velocities, fish interacted more over lateral motion (Fig. 5), predominantly swimming side-by-side in the Front region (Fig. 3). In contrast, in faster flows, they tended to favour an in-line formation next to the lateral walls (Fig. 3), promoting coordination through their longitudinal motion (Fig. 5). This phenomenon can be characterised as a "positioning bias", suggesting that the spatial distribution of fish within the environment significantly shapes their interactions.

Interestingly, intermediate velocity supported the highest correlations for both velocity components (Fig. 4a, and b), suggesting not only optimal exploration but also optimal coordination. This mirrors the J-shaped relationships between flow velocity and metabolic cost observed in various species<sup>45</sup> pointing to an optimal velocity where energetic efficiency and social cohesion converge. Although our design was limited to three flow velocities, these findings suggest the potential for an optimal flow regime for locomotion and interactions - insights that would be critical to fishway design. Future studies using a finer velocity range could clarify how interaction, exploration, and metabolic efficiency co-vary under changing flows.

Cross-correlation functions (Fig. 6) revealed bidirectional interaction in longitudinal motion, as depicted by the nearly symmetrical double peaks (Fig. 6a). Surprisingly, this bidirectionality persisted even at the highest flow velocity ( $U_{B35}$ ), where fish were mostly in-line (Fig. 2). In this arrangement, the Rear fish likely responds to the Lead fish's longitudinal motion (i.e. peak in  $C_u(\tau)$  for positive  $\tau$ ) via visual cues. Interestingly, the Lead fish also appeared to respond to the Rear fish (i.e. peak of  $C_u(\tau)$  for negative  $\tau$ ), may suggest sensory feedback through the lateral line system. Cyprinids possess numerous superficial neuromasts along the tail fin<sup>46</sup> which enable the detection of subtle hydrodynamic gradients. However, at elevated flows, such sensory feedback may

be disrupted by turbulence and flow disturbances<sup>11,24</sup>. Video recordings showed occasional collisions between the Rear and Lead fish, which may have triggered this bidirectional response.

Conversely, interaction over the lateral motion was largely unidirectional, with the Rear fish primarily responding to the Lead one (Fig. 6b). Notably, lateral response time decreased with increasing flow velocity, suggesting heightened responsiveness or alertness in fast-flow conditions. This observation aligns with known physiological stress responses<sup>47</sup> and altered behavioural states under elevated flow velocities<sup>48,49</sup>. These results suggest that extreme flows may not only challenge physical performance but also modulate sensory and behavioural processing.

It is important to acknowledge that linear correlation analysis has inherent limitations. It cannot depict the non-linear relationships often encountered in animal interactions<sup>50</sup> nor can it establish causality or precisely quantify information transfer. Nonetheless, correlation coefficients remain widely used due to their simplicity, interpretability, and utility in revealing broad patterns of animal interactions<sup>13,14</sup>. Future research could apply more sophisticated non-linear approaches, such as transfer entropy or machine learning techniques, to explore aspects of collective behaviour beyond the scope of the present study, including distinguishing among sensory modalities (e.g., visual, hydrodynamic, or acoustic cues) and quantifying directional information transfer.

All the findings in this work complement and extend previous research by showing that hydrodynamics and spatial layout are crucial yet often overlooked factors in fish collective behaviour studies. By examining fish interaction dynamics under ecologically relevant flows and with spatial boundaries, we highlight the risk of misinterpretation when omitting such factors, especially given that fish often swim near riverbanks or hard surfaces like fishway walls<sup>25–27</sup>.

From a modelling perspective, this study provides empirical parameters essential for developing ABMs of upstream collective migration<sup>51,52</sup>. These include formation patterns (Figs. 2 and 3), as well as decoupled coordination parameters for lateral and longitudinal motions – namely, interaction ranges (Fig. 4), boundary effects (Fig. 5), and response times (Fig. 6). As conservation efforts increasingly rely on model-driven design, integrating evidence-based rules – such as the effect of flow velocity and boundaries on fish collective behaviour – can significantly enhance the simulation performance and applicability of these tools<sup>3</sup>. This is particularly pertinent in fish passages, where knowledge of fish behavioural patterns is essential to ensure high passage efficiency<sup>53</sup>.

These results contribute to a broader understanding of how fish cope with high-flow environments through individual physiological adaptations and modulated collective behaviour. This behavioural plasticity may be a key component of resilience in fragmented, fast-flowing habitats and a valuable reference for both conservation planning and bio-inspired swarm system design.

## Data availability

The data underlying the findings of this study are available upon request. Researchers interested in accessing the dataset supporting this study, including raw detections, tracked positions of fish pairs, and an Excel database containing experimental data (e.g., testing times, temperatures, fish size, and weight), can contact the corresponding authors.

Received: 29 May 2025; Accepted: 23 July 2025

Published online: 27 August 2025

## References

- Krause, J. & Ruxton, G. D. *Living in Groups. Transactional Analysis Journal* vol. 43 Oxford University Press, (2013).
- Li, L. et al. Vortex phase matching as a strategy for schooling in robots and in fish. *Nat. Commun.* **11**, 1–9 (2020).
- Mawer, R. et al. Individual based models for the simulation of fish movement near barriers: current work and future directions. *J. Environ. Manage.* **335**, 117538 (2023).
- Deinet, S. et al. The Living Planet Index (LPI) for migratory freshwater fish. 55 pp (2020).
- Berdahl, A. et al. Collective animal navigation and migratory culture: from theoretical models to empirical evidence. *Philos Trans. R Soc. B Biol. Sci* **373**, 20170009. (2018).
- Closs, G. P., Krkosek, M. & Olden, J. D. *Conservation of Freshwater Fishes* (Cambridge University, 2016).
- Mozzi, G., Manes, C., Nyqvist, D., Domenici, P., & Comoglio, C. Aggregation in riverine fish: A review from a fish passage perspective. *International School of Hydraulics*, 265–280. (2023)
- Allouche, S. & Gaudin, P. Effects of avian predation threat, water flow and cover on growth and habitat use by chub, leuciscus cephalus, in an experimental stream. *Oikos* **94**, 481–492 (2001).
- Shelton, D. S. et al. Collective behavior in wild zebrafish. *Zebrafish* **17**, 243–252 (2020).
- Hockley, F. A., Wilson, C. A. M. E., Graham, N. & Cable, J. Combined effects of flow condition and parasitism on shoaling behaviour of female guppies poecilia reticulata. *Behav. Ecol. Sociobiol.* **68**, 1513–1520 (2014).
- De Bie, J., Manes, C. & Kemp, P. S. Collective behaviour of fish in the presence and absence of flow. *Anim. Behav.* **167**, 151–159 (2020).
- Ashraf, I. et al. Simple phalanx pattern leads to energy saving in cohesive fish schooling. *Proc. Natl. Acad. Sci. U S A.* **114**, 9599–9604 (2017).
- Cavagna, A. et al. Scale-free correlations in starling flocks. *Proc. Natl. Acad. Sci.* **107**, 11865–11870 (2010).
- Katz, Y., Tunström, K., Ioannou, C. C., Huepe, C. & Couzin, I. D. Inferring the structure and dynamics of interactions in schooling fish. *Proc. Natl. Acad. Sci. U. S. A.* **108**, 18720–18725 (2011).
- Butail, S., Mwaffo, V. & Porfiri, M. Model-free information-theoretic approach to infer leadership in pairs of zebrafish. *Phys. Rev. E.* **93**, 42411 (2016).
- Porfiri, M. Inferring causal relationships in zebrafish-robot interactions through transfer entropy: a small lure to catch a big fish. *Anim. Behav. Cogn.* **5**, 341–367 (2018).
- Ko, H., Lauder, G. & Nagpal, R. The role of hydrodynamics in collective motions of fish schools and bioinspired underwater robots. *J. R Soc. Interface.* **20**, 20230357 (2023).
- Hensor, E., Couzin, I. D., James, R. & Krause, J. Modelling density-dependent fish shoal distributions in the laboratory and field. *Oikos* **110**, 344–352 (2005).

19. Magurran, A. E. & Pitcher, T. J. Provenance, shoal size and the sociobiology of predator-evasion behaviour in minnow shoals. *Proc. R Soc. Lond. Ser. B Biol. Sci.* **229**, 439–465 (1987).
20. Ashraf, I., Godoy-Diana, R., Halloy, J., Collignon, B. & Thiria, B. Synchronization and collective swimming patterns in fish (*Hemigrammus bleheri*). *J R Soc. Interface* **13**, 20160734 (2016).
21. Lombana, D. A. B. & Porfiri, M. Collective response of fish to combined manipulations of illumination and flow. *Behav. Processes.* **203**, 104767 (2022).
22. de Duarte, B. A., Ramos, I. C. R. & F. & Reynolds shear-stress and velocity: positive biological response of Neotropical fishes to hydraulic parameters in a vertical slot fishway. *Neotrop. Ichthyol.* **10**, 813–819 (2012).
23. Silva, A. T., Santos, J. M., Ferreira, M. T., Pinheiro, A. N. & Katopodis, C. Effects of water velocity and turbulence on the behaviour of Iberian Barbel (*Luciobarbus bocagei*, Steindachner 1864) in an experimental pool-type fishway. *River Res. Appl.* **27**, 360–373 (2011).
24. Chicoli, A. et al. The effects of flow on schooling *Devario aequipinnatus*: school structure, startle response and information transmission. *J. Fish. Biol.* **84**, 1401–1421 (2014).
25. Kerr, J. R., Manes, C. & Kemp, P. S. Assessing hydrodynamic space use of brown trout, *Salmo trutta*, in a complex flow environment: a return to first principles. *J. Exp. Biol.* **219**, 3480–3491 (2016).
26. Hughes, N. F. The wave-drag hypothesis: an explanation for size-based lateral segregation during the upstream migration of salmonids. *Can. J. Fish. Aquat. Sci.* **61**, 103–109 (2004).
27. Morán-López, R. & Tolosa, O. U. Obstacle negotiation attempts by leaping cyprinids indicate bank-side spawning migration routes. *Fish. Res.* **197**, 84–87 (2018).
28. Herbert-Read, J. E. et al. Inferring the rules of interaction of shoaling fish. *Proc. Natl. Acad. Sci.* **108**, 18726–18731 (2011).
29. Ward, A. J. W., Sumpter, D. J. T., Couzin, I. D., Hart, P. J. B. & Krause, J. Quorum decision-making facilitates information transfer in fish shoals. *Proc. Natl. Acad. Sci. U S A.* **105**, 6948–6953 (2008).
30. Schiavon, A. et al. Survival and swimming performance of a small-sized cypriniformes (*Telestes muticellus*) tagged with passive integrated transponders. *J. Limnol.* **82**, (2023).
31. Mozzi, G. et al. The interplay of group size and flow velocity modulates fish exploratory behaviour. *Sci. Rep.* **14**, 13186 (2024).
32. Ashraf, M. U. et al. Fish swimming performance: effect of flume length and different fatigue definitions. *Int. School Hydraul.*, 1–11 (2023)
33. Redmon, J., Divvala, S., Girshick, R. & Farhadi, A. You only look once: Unified, real-time object detection. in *Proceedings of the IEEE conference on computer vision and pattern recognition* 779–788 (2016).
34. Pearson, K. VII. Note on regression and inheritance in the case of two parents. *Proc. R Soc. Lond.* **58**, 240–242 (1895).
35. R Core Team. R: A Language and Environment for Statistical Computing. at (2022). <https://www.r-project.org/>
36. Wickham, H. *Ggplot2: Elegant Graphics for Data Analysis* (Springer-, 2016).
37. Kassambara, A. & rstatix Pipe-Friendly Framework for Basic Statistical Tests. at (2023). <https://rpkgs.datanovia.com/rstatix/>
38. Friedman, M. The use of ranks to avoid the assumption of normality implicit in the analysis of variance. *J. Am. Stat. Assoc.* **32**, 675–701 (1937).
39. Percie, D. et al. The ARRIVE guidelines 2.0: updated guidelines for reporting animal research. *BMJ Open. Sci.* **4**, 1769–1777 (2020).
40. Garner, P. Effects of variable discharge on the velocity use and shoaling behavior of *Phoxinus Phoxinus*. *J. Fish. Biol.* **50**, 1214–1220 (1997).
41. Fish, F. E. Swimming strategies for energy economy. *Fish. Locomot Eco-ethological Perspect.* 102–134. <https://doi.org/10.1201/b10190> (2010).
42. Liao, J. C. A review of fish swimming mechanics and behaviour in altered flows. *Philos. Trans. R Soc. B Biol. Sci.* **362**, 1973–1993 (2007).
43. Grossman, G. D., Rincon, P. A., Farr, M. D. & Ratajczak, R. E. A new optimal foraging model predicts habitat use by drift-feeding stream minnows. *Ecol. Freshw. Fish.* **11**, 2–10 (2002).
44. Schumann, S. et al. Social buffering of oxidative stress and cortisol in an endemic cyprinid fish. *Sci. Rep.* **13**, 20579 (2023).
45. Di Santo, V., Kenaley, C. P. & Lauder, G. V. High postural costs and anaerobic metabolism during swimming support the hypothesis of a U-shaped metabolism–speed curve in fishes. *Proc. Natl. Acad. Sci. U S A.* **114**, 13048–13053 (2017).
46. Beckmann, M., Erős, T., Schmitz, A. & Bleckmann, H. Number and distribution of superficial neuromasts in twelve common European cypriniform fishes and their relationship to habitat occurrence. *Int. Rev. Hydrobiol.* **95**, 273–284 (2010).
47. Pottinger, T. G. The stress response in fish—mechanisms, effects and measurement. *Fish Welf* 32–48 (2008).
48. Zelnik, P. R. & Goldspink, G. The effect of exercise on plasma cortisol and blood sugar levels in the rainbow trout, *Salmo gairdnerii* Richardson. *J. Fish. Biol.* **19**, 37–43 (1981).
49. Li, X. et al. Effect of flow velocity on the growth, stress and immune responses of turbot (*Scophthalmus maximus*) in recirculating aquaculture systems. *Fish. Shellfish Immunol.* **86**, 1169–1176 (2019).
50. Couzin, I. D. & Krause, J. Self-Organization and collective behavior in vertebrates. *Adv. Study Behav.* **32**, 1–75 (2003).
51. Milner-Gulland, E. J., Fryxell, J. M. & Sinclair, A. R. E. *Animal Migration: A Synthesis* OUP Oxford., (2011).
52. Couzin, I. D. Collective animal migration. *Curr. Biol.* **28**, R976–R980 (2018).
53. Noonan, M. J., Grant, J. W. A. & Jackson, C. D. A quantitative assessment of fish passage efficiency. *Fish. Fish.* **13**, 450–464 (2012).

## Acknowledgements

The authors express gratitude to A. Cagninei and R. Bosio for their assistance in laboratory activities, and M. U. Ashraf, D. Nyqvist and S. Schumann for their support during the experimental activities. We thank P. Lo Conte for supporting field operations during electrofishing and providing technical advice throughout the experimental campaign. Appreciation is extended to the Incubatoio di Porte di Pinerolo for hosting and facilitating our experiments.

## Author contributions

Conceptualisation: G.M., C.M.; methodology: G.M., C.M.; formal analysis: G.M.; investigation: G.M.; Writing-original draft: G.M.; Writing-review & editing: G.M., C.C., C.M.; Visualisation: G.M.; supervision: C.C., C.M.; project administration and funding acquisition: C.C.; Validation: C.M., Software: G.M. All authors reviewed and approved the final manuscript.

## Funding

The research work was carried out with funding received from the European Union Horizon 2020 Research and Innovation Programme under the Marie Skłodowska-Curie Actions, Grant Agreement No. 860800.

## Declarations

### Competing interests

The authors declare no competing interests.

### Additional information

**Supplementary Information** The online version contains supplementary material available at <https://doi.org/10.1038/s41598-025-13332-5>.

**Correspondence** and requests for materials should be addressed to G.M.

**Reprints and permissions information** is available at [www.nature.com/reprints](http://www.nature.com/reprints).

**Publisher's note** Springer Nature remains neutral with regard to jurisdictional claims in published maps and institutional affiliations.

**Open Access** This article is licensed under a Creative Commons Attribution-NonCommercial-NoDerivatives 4.0 International License, which permits any non-commercial use, sharing, distribution and reproduction in any medium or format, as long as you give appropriate credit to the original author(s) and the source, provide a link to the Creative Commons licence, and indicate if you modified the licensed material. You do not have permission under this licence to share adapted material derived from this article or parts of it. The images or other third party material in this article are included in the article's Creative Commons licence, unless indicated otherwise in a credit line to the material. If material is not included in the article's Creative Commons licence and your intended use is not permitted by statutory regulation or exceeds the permitted use, you will need to obtain permission directly from the copyright holder. To view a copy of this licence, visit <http://creativecommons.org/licenses/by-nc-nd/4.0/>.

© The Author(s) 2025